

# Lawrence Berkeley National Laboratory

## Recent Work

### Title

TESTING THE MAGNETIC FIELD OF THE BEVATRON

### Permalink

<https://escholarship.org/uc/item/6tk9d7nn>

### Author

Lambertson, Glen R.

### Publication Date

1955-11-10

UNIVERSITY OF  
CALIFORNIA

*Radiation  
Laboratory*

TWO-WEEK LOAN COPY

*This is a Library Circulating Copy  
which may be borrowed for two weeks.  
For a personal retention copy, call  
Tech. Info. Division, Ext. 5545*

BERKELEY, CALIFORNIA

## **DISCLAIMER**

This document was prepared as an account of work sponsored by the United States Government. While this document is believed to contain correct information, neither the United States Government nor any agency thereof, nor the Regents of the University of California, nor any of their employees, makes any warranty, express or implied, or assumes any legal responsibility for the accuracy, completeness, or usefulness of any information, apparatus, product, or process disclosed, or represents that its use would not infringe privately owned rights. Reference herein to any specific commercial product, process, or service by its trade name, trademark, manufacturer, or otherwise, does not necessarily constitute or imply its endorsement, recommendation, or favoring by the United States Government or any agency thereof, or the Regents of the University of California. The views and opinions of authors expressed herein do not necessarily state or reflect those of the United States Government or any agency thereof or the Regents of the University of California.

UCRL-2818  
Unclassified Physics

*cy 3.*

UNIVERSITY OF CALIFORNIA  
Radiation Laboratory  
Berkeley, California  
Contract No. W-7405-eng-48

TESTING THE MAGNETIC FIELD OF THE BEVATRON

Glen R. Lambertson

November 10, 1954

TESTING THE MAGNETIC FIELD OF THE BEVATRON

Contents

Abstract . . . . .	3
Introduction . . . . .	4
Equipment and Procedures	
Positioning Gear . . . . .	5
Residual Field Measurement . . . . .	5
Integrator; Signal Programming and Recording System . . . . .	8
Kidney Coils . . . . .	15
Boom Coil . . . . .	15
n-Coils . . . . .	19
Verticality Coils . . . . .	19
Special Surveys . . . . .	20
Description of the Bevatron Magnet Field	
Average Flux Density . . . . .	21
Radial Variation of Flux Density . . . . .	21
Effect of Pole-Face-Windings at High B . . . . .	27
Median Surface . . . . .	27
Miscellaneous . . . . .	27
Summary . . . . .	28
Acknowledgments . . . . .	29

## TESTING THE MAGNETIC FIELD OF THE BEVATRON

Glen R. Lambertson

Radiation Laboratory, Department of Physics  
University of California, Berkeley, California

November 10, 1954

### ABSTRACT

The significant features of the bevatron magnetic field were examined in a program of magnetic measurements. Studies of the pulsed field employed an electronic integrator with special search coils. An oscilloscope pattern presenting data at about thirty magnet-current values per magnet pulse was photographically recorded. Although many new details were discovered, the behavior of the bevatron magnet was found to be consistent with model predictions. Some changes in the field distribution were necessary, but generally the magnet must be regarded as very satisfactory.

## TESTING THE MAGNETIC FIELD OF THE BEVATRON

Glen R. Lambertson

Radiation Laboratory, Department of Physics  
University of California, Berkeley, California

November 10, 1954

### INTRODUCTION

Upon completion of the bevatron magnet, a magnetic field measurement program was conducted. The purposes were to determine the suitability of the field for particle acceleration, to make modifications as seemed advisable, and to provide data for calculating particle behavior in connection with beam acceleration and deflection. To meet these requirements involved an extensive survey of the dependence of flux density upon radius, azimuth, and magnet current.

A full pulse of current in the bevatron magnet produces a field which rises at an approximately uniform rate of 9,000 gauss/sec to a peak of 15,500 gauss. The field was studied at selected values of magnet current during the rising portion of the pulse. Most of the testing procedure was concerned with obtaining information on values of  $n$ , the median surface, and the total flux density,  $B$ . The term  $n$  is defined as a function of the radial gradient of the axial component of the flux density,

$$n = - \frac{R}{B} \frac{\partial B}{\partial R}$$

and in the bevatron  $n$  has a nominal value of 0.6. Axial focusing forces on the proton are directed toward the median surface; this surface is defined by those points at which the flux density has zero radial component.

A basic measuring system consisting of search coil, electronic integrator, and oscilloscope was chosen for the pulsed-field tests. These components can be constructed having the frequency response and precision required for measuring the pulsed field with an accuracy better than 1%. The flexibility afforded by use of search coils designed for special purposes, plus the further advantages of using balanced opposing coils for measuring field differences, made the search coil a very valuable tool for the bevatron measurement program.

The testing program, completed in December 1953, required two months of bevatron magnet operation. The first two weeks of this period were devoted to assuring ourselves of the proper functioning and adjustment of the measurement apparatus as used in the bevatron. Photographic recording of the data allowed rapid progress through the more routine and detailed measurements that followed. Only a minimum amount of data reduction necessary to the progress of the program was carried out concurrent with the data recording. Small corrections to the bevatron field were applied and checked during the two-month period.

## EQUIPMENT AND PROCEDURES

### A. Positioning Gear

The bevatron magnet is composed of four  $90^\circ$  quadrants separated by 20-foot straight sections. Each quadrant contains 36 wedge-shaped units called sectors; a simplified view of a typical sector is shown in Fig. 1. The designations of the sectors and their relative positions are shown in Fig. 2, which is a diagram of the geometric plan of the bevatron magnet.

To provide a convenient positioning system for search coils and probes, three carts constructed of nonmagnetic and largely nonmetallic materials were placed in the magnet gap on temporary wooden rails. Control strings from a cart to an operator outside the magnet allowed him to move the cart; a coil carriage on each cart provided radial motion, which also was controlled by strings from outside the magnet. Each cart and each carriage was provided with detents that determined azimuthal stops at the sector centers and radial positions at 3-inch intervals.

The carts were provided with an indicating system to give the position of a probe in terms of sector number and radial position. This system was based on simple variable-resistance circuits with dc microammeters to show probe positions. One set of these meters was mounted on a data board, which was photographed once each bevatron pulse with the recording camera. Two other sets of meters were provided for the use of the measurement equipment operators.

### B. Residual Field Measurement

The choice of integrator and search coils for the pulsed-field measurements made necessary a separate measurement of the magnet's residual field. For this purpose, an "rf magnetometer" (see print 3V8351) was used. This instrument contains a small needle of permalloy which acts as the core of an rf transformer. A simple harmonic input current is supplied and the magnetic nonlinearity of the permalloy produces a distorted voltage wave form at the transformer output; this output is analyzed for second harmonic content. When the average flux density about the permalloy is zero, the hysteresis loop is symmetric and the output contains no second harmonic. A biasing solenoid, coaxial with the permalloy needle, is provided to cancel the effect of an externally applied field; the solenoid current required to null the second harmonic signal is thus a measure of that external field. In the rf magnetometer, the bias solenoid current is controlled by the second harmonic detector and the instrument provides a continuous measurement of flux density.

The magnetometer was used with a Speedomax recording potentiometer, and the bevatron axial residual field,  $B_z$ , of about 33 gauss was measured to 1%. For azimuthal runs at selected radii, the recorder chart drive motor was operated continuously as the probe was carried, on the cart, through the quadrant; radial runs with 3-inch radial intervals were made across the azimuthal runs to complete the survey inside the quadrants. For a detailed survey of the fringing regions and straight sections, the magnetometer probe was positioned manually at points on a reference grid covering those areas.



(FILE NO. 15370-1)

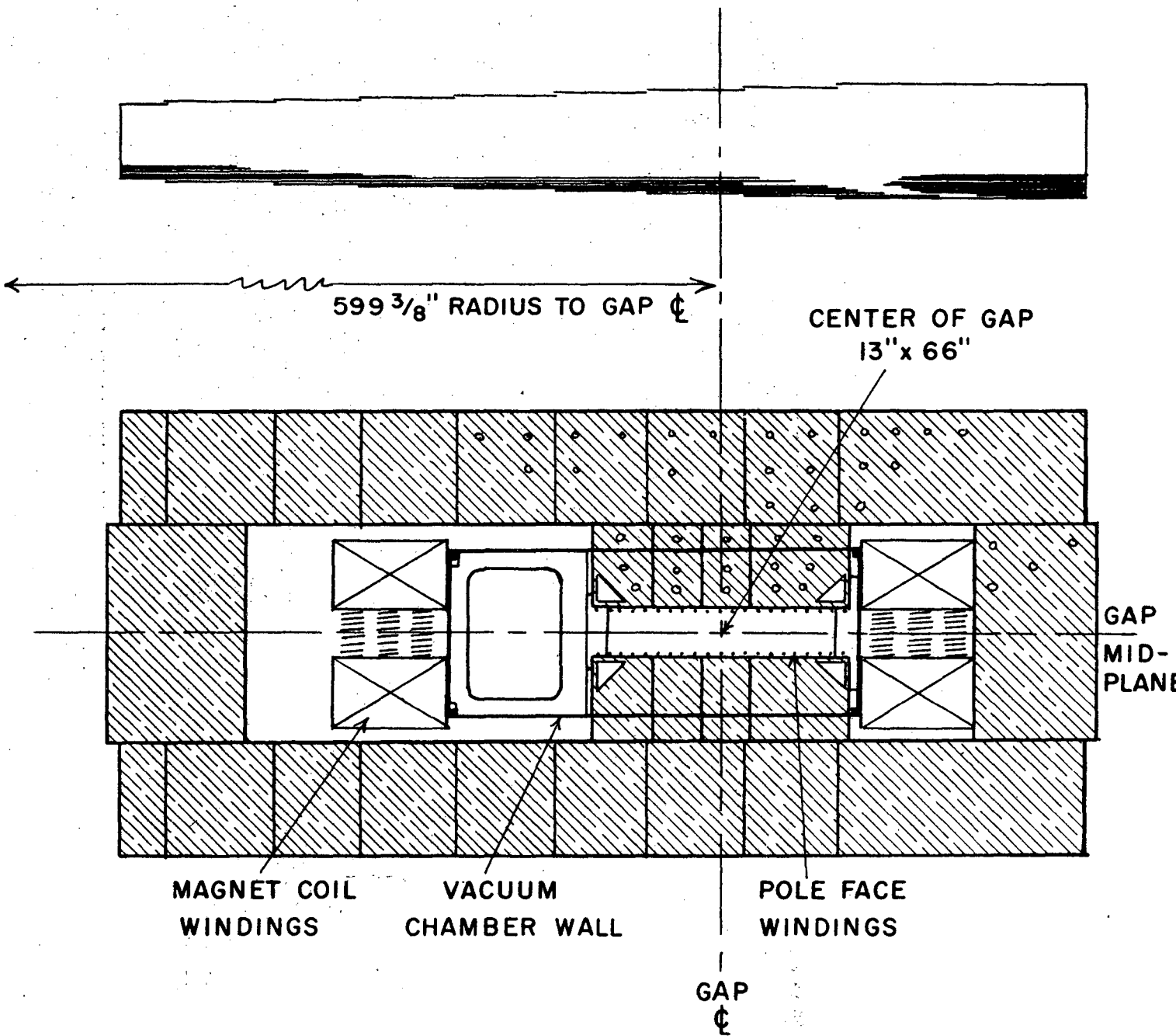


FIG. 1 A SECTOR OF THE BEVATRON MAGNET

(FILE NO. 15370-2)

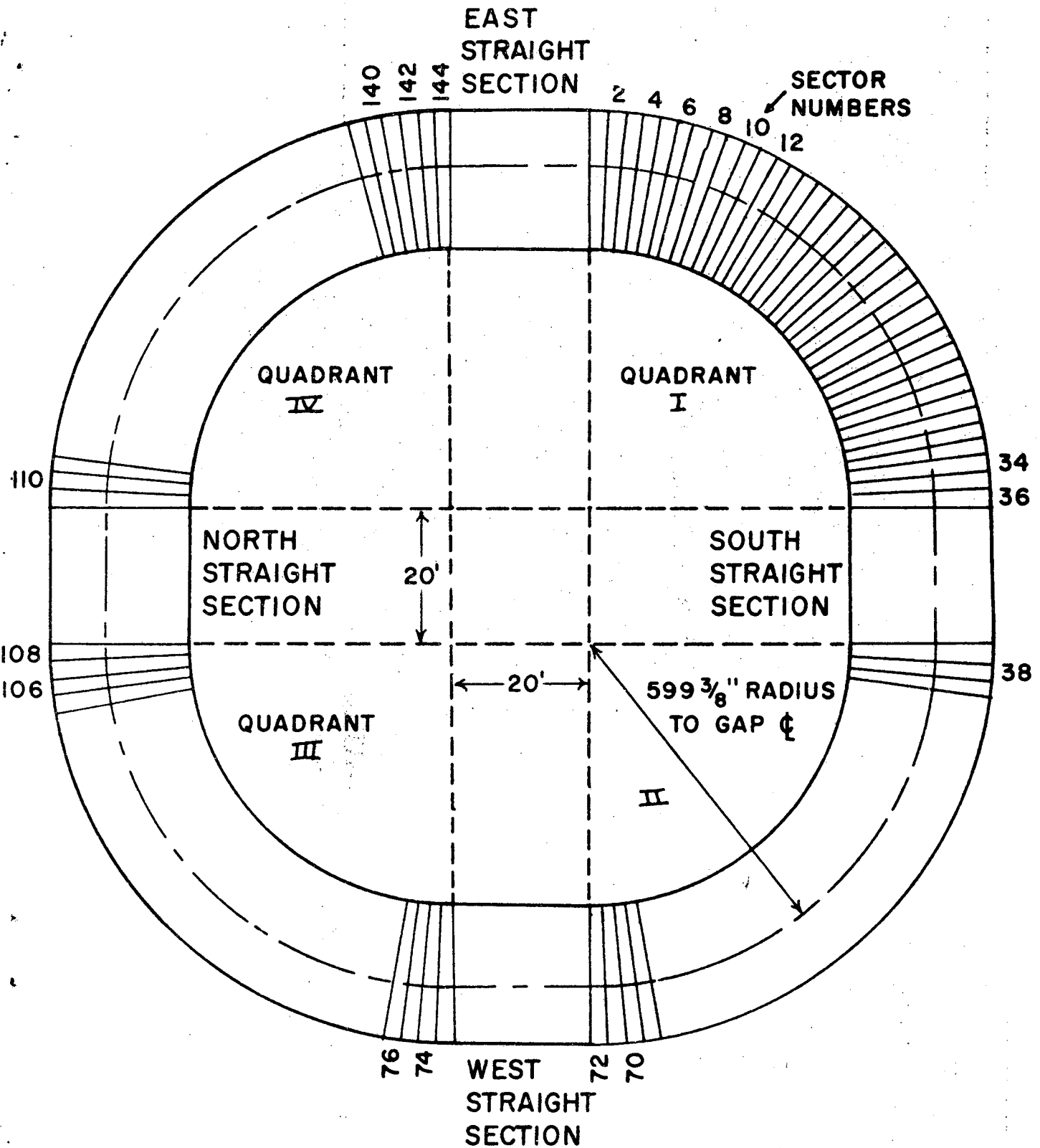


FIG. 2 LOCATIONS OF SECTORS IN BEVATRON

The dependence of residual field upon magnet history required that the pulsing conditions before a measurement be standardized to those used throughout the tests of dynamic field.

The radial component of the residual field was measured with the rf magnetometer with its probe axis horizontal. An accuracy of  $\pm 0.01$  gauss was desired, requiring that the probe be held within  $3 \times 10^{-4}$  radians of horizontal; this precision in direction was attained by mounting the probe on a lucite form which was then floated on a mercury pool. The direction, with respect to horizontal, of the sensitive axis of the probe was experimentally adjusted to within the desired tolerance, using small weights to displace the center of mass of the floating system. With periodic inspection and readjustment, this apparatus was used to measure the radial component at about 800 places in the magnet gap.

### C. Integrator and Signal Programming and Recording System

The electronic integrator in use for general magnetic measurement work\* was suitable for the bevatron application; the requirements called for a dc integrator with response to about ten kilocycles/second and accuracy over a broad range of output signal. The need for frequent adjustment to remove integrator-output drift led to the construction of a servomechanism that continuously corrected and maintained the drift adjustment during stand-by periods. It was necessary to disable this balance servo while the integrator was in use, and a circuit was provided to do this automatically when the bevatron was pulsed. With these auxiliaries, the integrator required comparatively little attention from the equipment operator. Integrator RC combinations of 0.2 sec and 0.06 sec were used in the measurements.

Much of the electronic measuring equipment would be seriously affected by a strong pulsed stray field; accordingly, a location for this equipment was chosen about 70 feet from the bevatron magnet where a stray field of only 5 to 10 gauss would appear. This remote location required that the signal circuits from the pickup coils be carefully planned to avoid adverse effects of cable capacitance, noise pickup, and ground currents. A single electrical ground was established at the integrator and all the circuits were tied to this point; closed loops in which currents might be induced were avoided. For protection of personnel and equipment against accidental connection of the probes to a high voltage, extra insulation was added to the cables leading to the carts and all conductors of these cables came through fuse-and-spark-gap assemblies before entering a mixing circuit at the center of the magnet. From the magnet center to the integrator, special cables were installed for the integrator signals and position-indicator signals.

The oscilloscope used to display the integrator signal needed good photographic qualities, small spot size, stable amplifiers, and insensitivity to stray fields. At the time the measurement equipment was being planned, no available oscilloscope was satisfactory; a Tektronix 513 D oscilloscope equipped with a 5XP11 type cathode ray tube was modified for the job. Its horizontal-deflection system was employed for the integrator output signal because a broader usable screen width was permitted on this axis. Overall resolution better than 0.6% of the usable screen width was obtained with reasonable stability; the need for long-time stability of the oscilloscope

\*R. Madey and G. Farly, "An Electronic Voltage Integrator", Rev. Sci. Instr. 25, 275 (1954).

system was removed by frequent calibrations of the apparatus during the measurements. A magnetic shield enclosing the oscilloscope was built of annealed iron sheet and the spot deviation resulting from the stray field was reduced to a few tenths of a millimeter.

The bevatron current-monitoring system delivers a marker signal at each of 32 values of magnet current during a magnet pulse; the magnetic field was measured at each of these current markers. The pulsed flux densities to be measured ranged from 250 gauss to 16,000 gauss; accuracies of 0.5% were desired in the measurement of total field. To obtain this precision with an oscilloscope having a resolution of 0.6% full screen, the integrator output signal was biased so that the minimum over-all precision of the scope deflection plus known zero-depressing (biasing) voltage was the desired 0.5% of the total signal. Further signal programming was necessary to provide continuous monitoring of the signal as it increased above the injection value. Because the field rises steadily, the signal could be kept on the oscilloscope screen by successive attenuations at the proper moments; seven attenuations were used, each decreasing the signal by a factor of about 1.68. An oscilloscope sweep signal, logarithmic in time, spaced the successive signal traces evenly across the CRT screen. The current markers were shown as intensified pips on the fainter signal traces. These signal-programming and display functions were electronically controlled and repeated automatically, if desired, for each bevatron pulse. Figure 3 is a photograph of the oscilloscope pattern received with this programming of the integrated signal from a single coil in the bevatron field; in Fig. 4, the signal difference from two opposed pickup coils is recorded without zero-depress voltage. Each oscillogram has a single horizontal trace at the center showing the output voltage of the integrator just before the bevatron pulse began.

To calibrate the integrator, signal programmer, and oscilloscope as used, a known calibrating voltage was connected by mercury relay to the integrator input; this calibrating voltage was adjusted to give a scope pattern similar to a full field pulse except that it had time markers in place of the bevatron current markers. The equivalent value in flux of each time mark was calculable from the calibrating voltage and the elapsed time. This time-pip calibrating cycle, like the measurement cycle, proceeded automatically from a single initiating signal and provided a rapid and convenient dynamic calibration of the complete system. A time-pip calibration is shown in Fig. 5.

An auxiliary calibrating cycle, which covered the oscilloscope screen with a grid of horizontal lines, equally spaced in terms of integrator input, was also provided; this scheme showed the nonlinearities in the system but was of limited value compared with the time-pip type.

A stereoscopic camera built for making cloud chamber photographs was adapted to the needs of the bevatron magnetic measurements. One lens photographed the oscilloscope screen and the other lens made a record of the meters, counters, and notes on the data board; Fig. 6 is a picture of the data board taken with this camera. Figure 7 shows the data board, oscilloscope, and camera shutter and mount with camera removed. The camera operated automatically as a part of the recording cycle. Data were read from the film by optically projecting the photograph of the current pips upon a scale prepared from time-pip-type calibrations.



Fig. 3. Photographic record of measurement using one kidney coil.

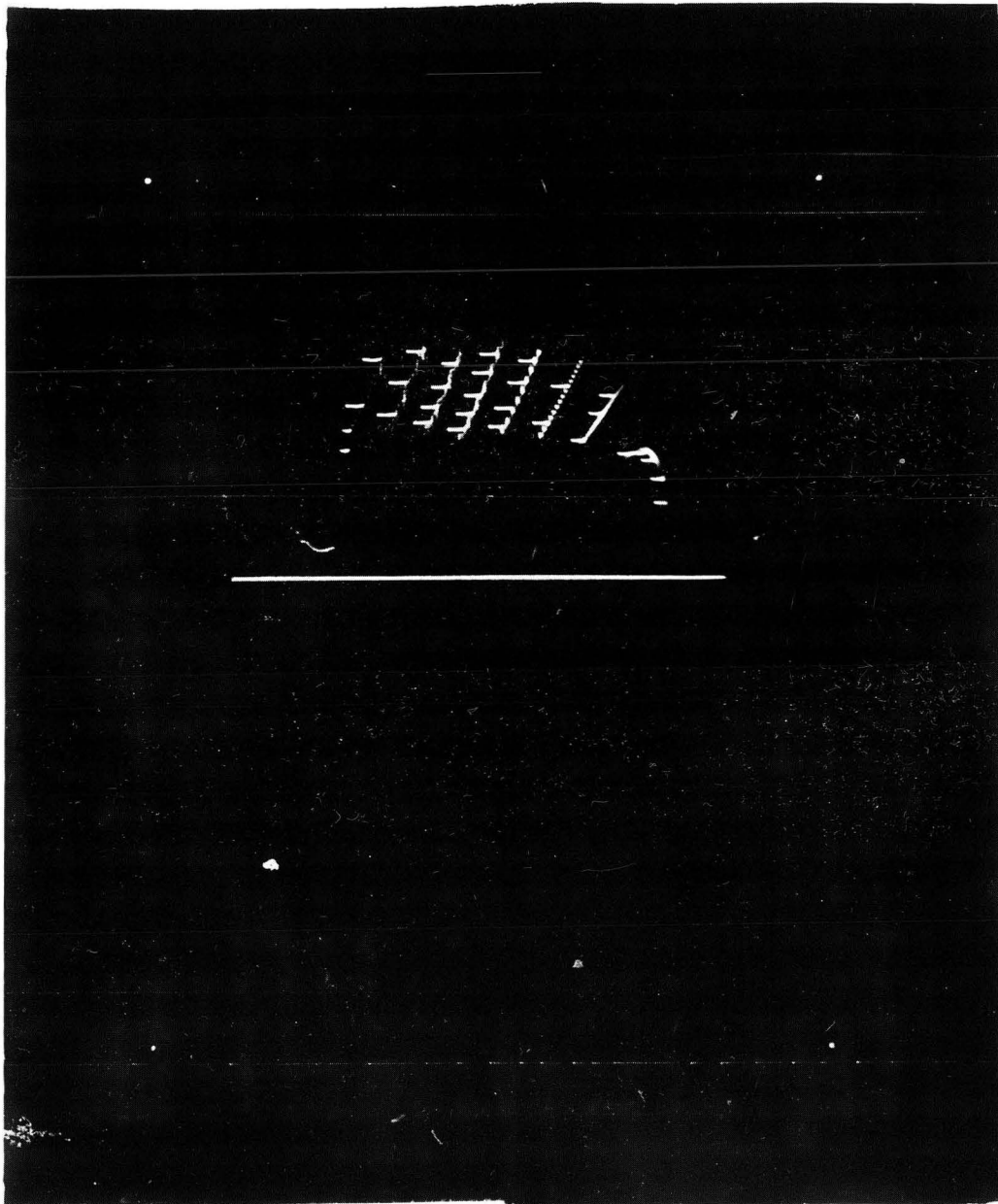


Fig. 4. Photographic record of measurement using opposed coils.

Z N - 1160

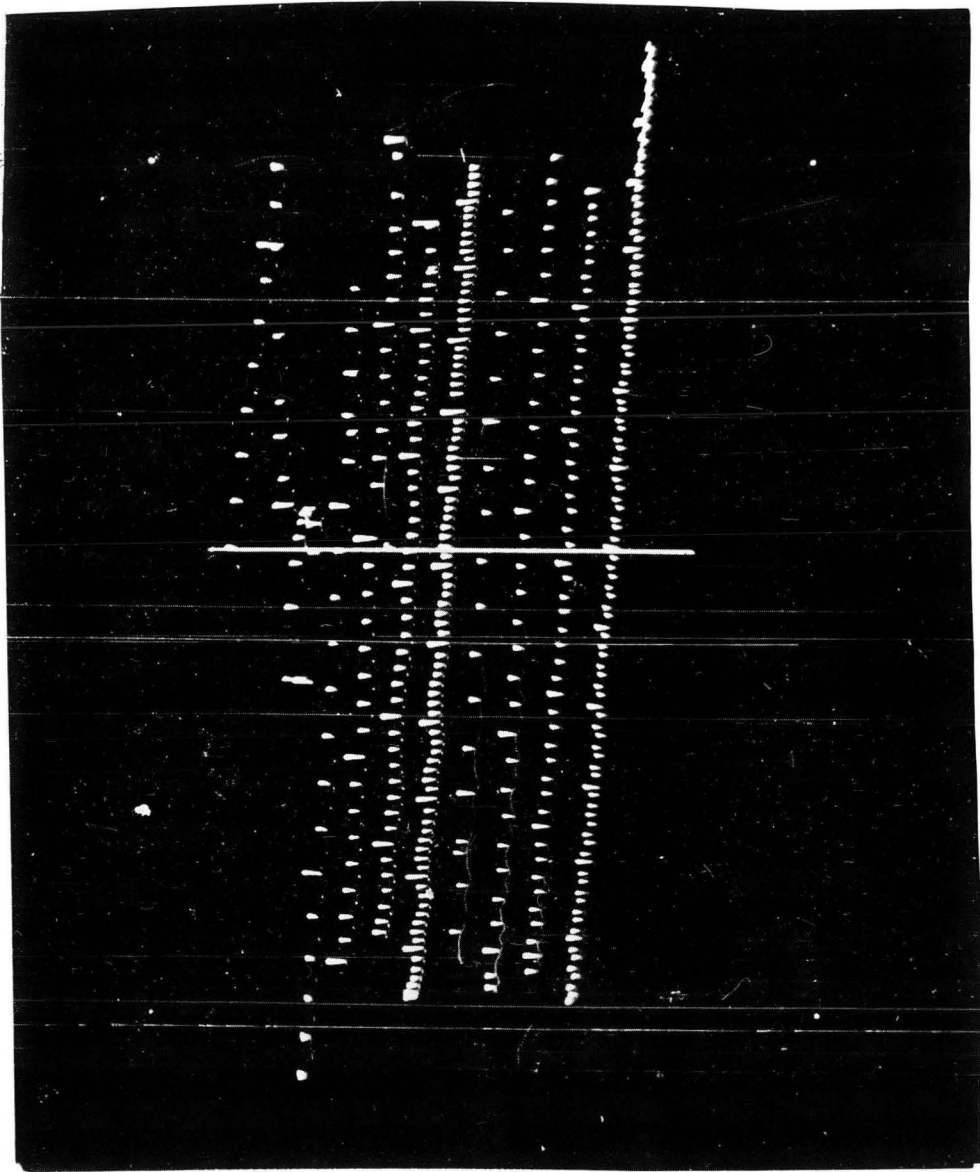


Fig. 5. A time-pip calibration.

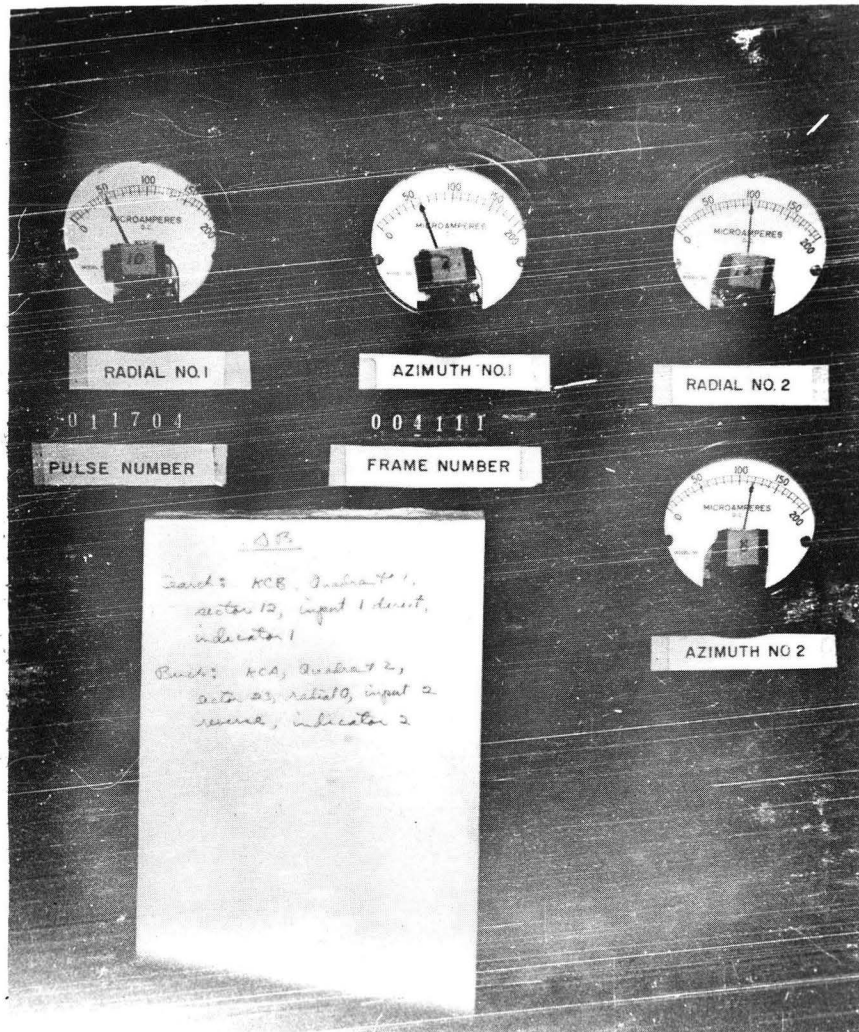


Fig. 6. Data-board photograph.

ZN-1162



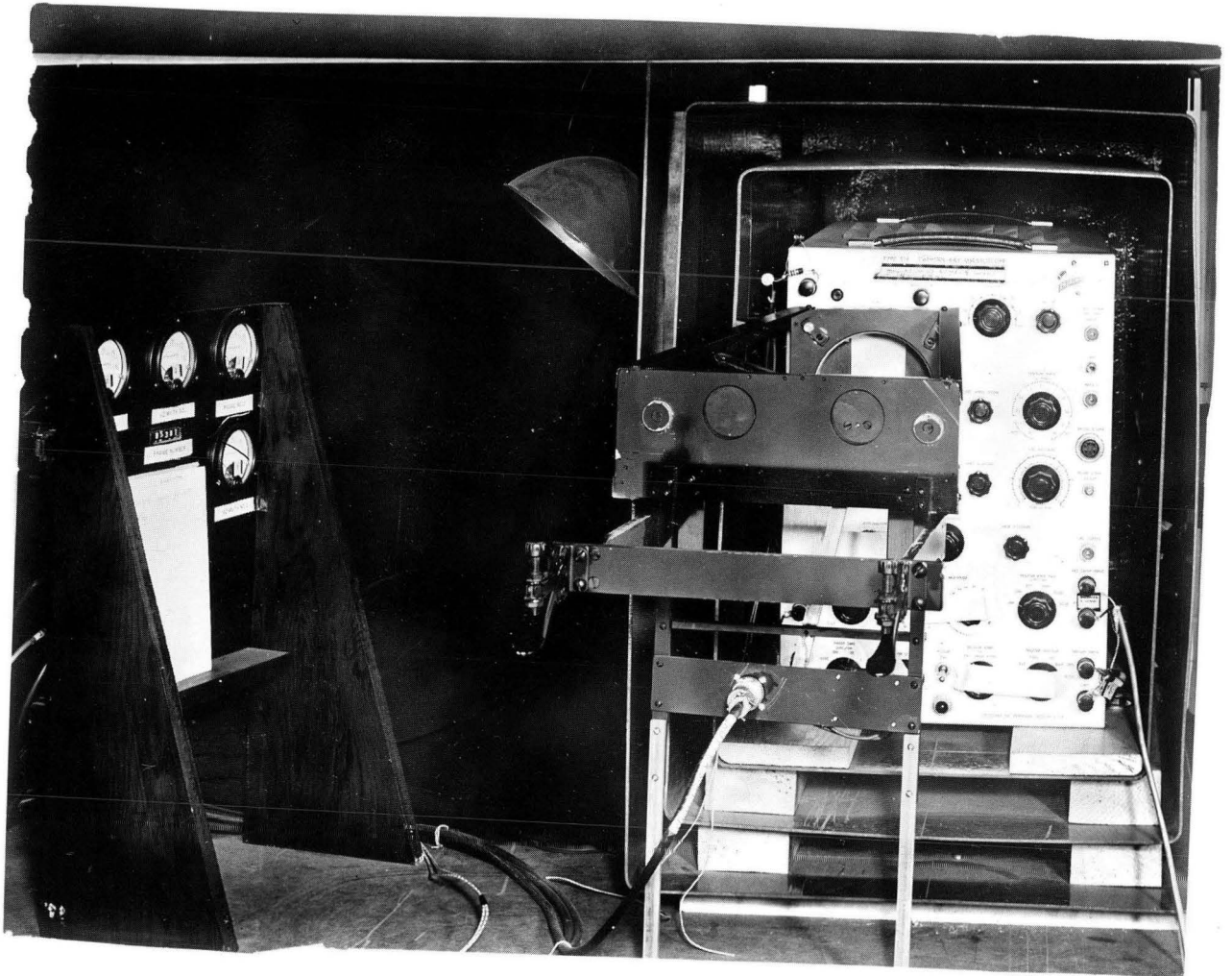


Fig. 7. Data board and oscilloscope with camera mount.

ZN-1163

The complete signal programming and recording system contained many elements; a block diagram is given in Fig. 8 and the physical appearance is shown in Fig. 9. Although tedious to design and construct, this system was very satisfactory in operation. Most of the automatic features were required by the nature of the problem; the remainder served to prevent loss of data through human error. About 5,000 pulses were photographed; most of these pictures contained thirty or more field measurements each.

#### D. Kidney Coils

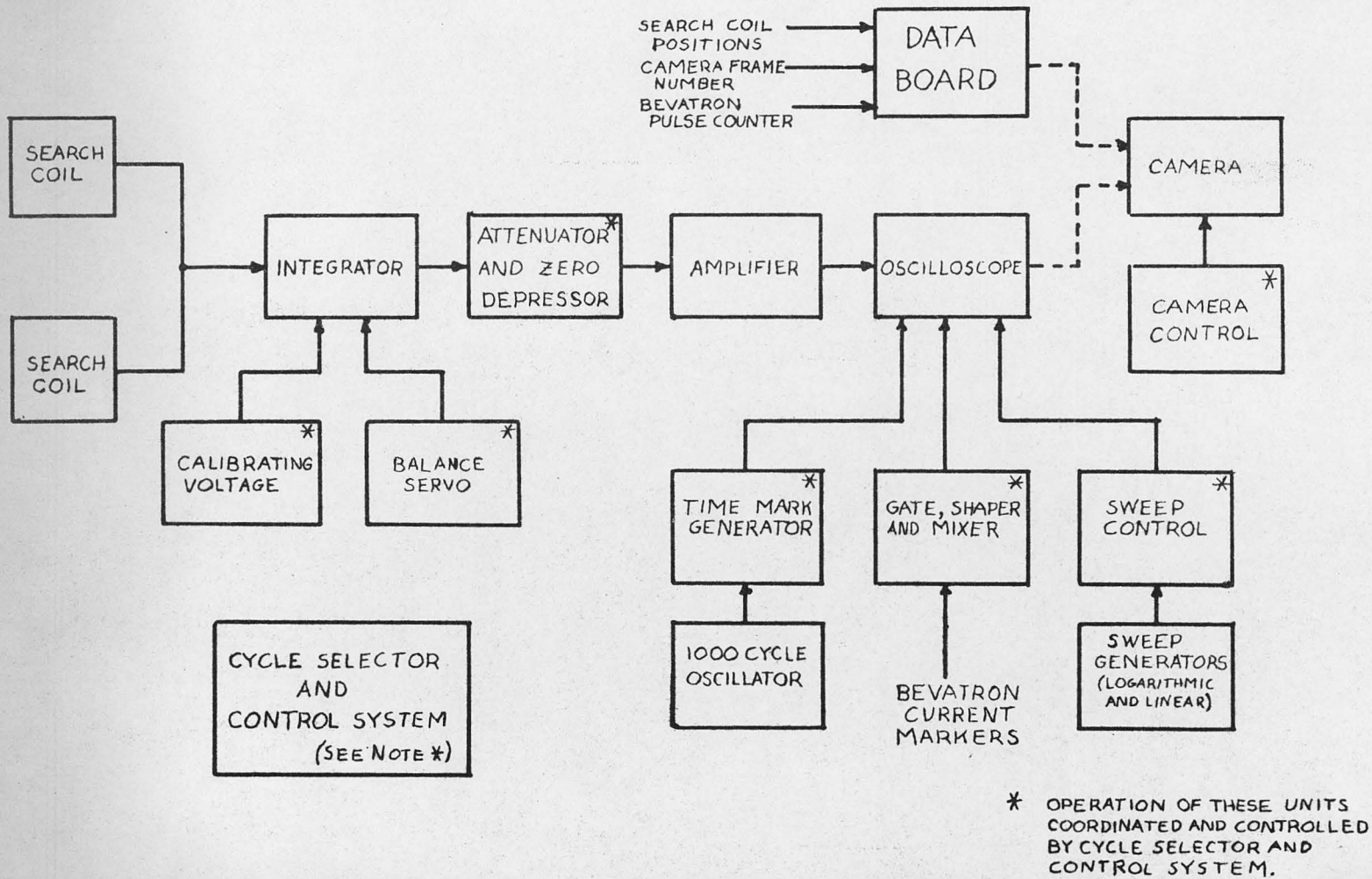
The number of measurements required to survey the field azimuthally was reduced by employing search coils that extended azimuthally over 52.3 inches, the length of two sectors, in the bevatron magnet. Two coils were made on carefully constructed bakelite forms and precision wound so that their effective turns-area values were calculable from measured dimensions. A sketch of the construction of these "kidney" coils is shown in Fig. 10; each was two inches wide radially and curved with the 599-3/8-inch radius of the gap centerline. Constructing these coils in a manner allowing geometric determination of their areas within 0.1% was chosen in preference to attempting a magnetic measurement of their areas. The total area of a kidney coil was  $2 \times 10^5$  turns-cm<sup>2</sup>, with a tap at one-eighth of this area. The areas of the two completed coils were compared magnetically and made equal by adjusting the area of one coil; it is of interest that the two coils as initially constructed differed in area by less than 0.015%.

The one-eighth-area tap of a kidney coil was connected directly to the integrator for total dynamic field measurement. For field differences, two kidney coils with the signals from their total areas connected in series-opposing were used; with this system, field differences of 0.01% were measurable. In use, the kidney coil was placed with its center on a sector centerline, its ends extending on either side into the adjacent sectors. The azimuthal gradient of flux density is generally lowest at midsector; placement of the coil with its ends in these regions made the measurement less sensitive to error in coil location.

#### E. Boom Coil

The boom coil was designed for the special purpose of yielding, in a single measurement, the integral of the flux density through the fringing regions at the straight sections. Similar in construction to the kidney coil, the boom coil was two inches wide and long enough to extend through the 20-foot straight section and 2-1/2 sectors into each adjacent quadrant. This length, although awkward to handle, was chosen because it placed the ends of the coil in similar fields with relatively small azimuthal gradients; as in the case of the kidney coil, this condition reduced the sensitivity to azimuthal displacements of the coil. Because it was expected that the field covered by the boom coil would be about equivalent to that in five sectors at midquadrant, the turns-width product of the boom coil was made two-fifths that of a kidney coil. A kidney coil at midquadrant was then connected series-opposing, to provide the greater relative precision of difference measurements in the study of radial variation of the fringing field.

(FILE NO. 15370-6)



SCHEMATIC DIAGRAM OF PULSED-FIELD MEASUREMENT SYSTEM

FIG. 8

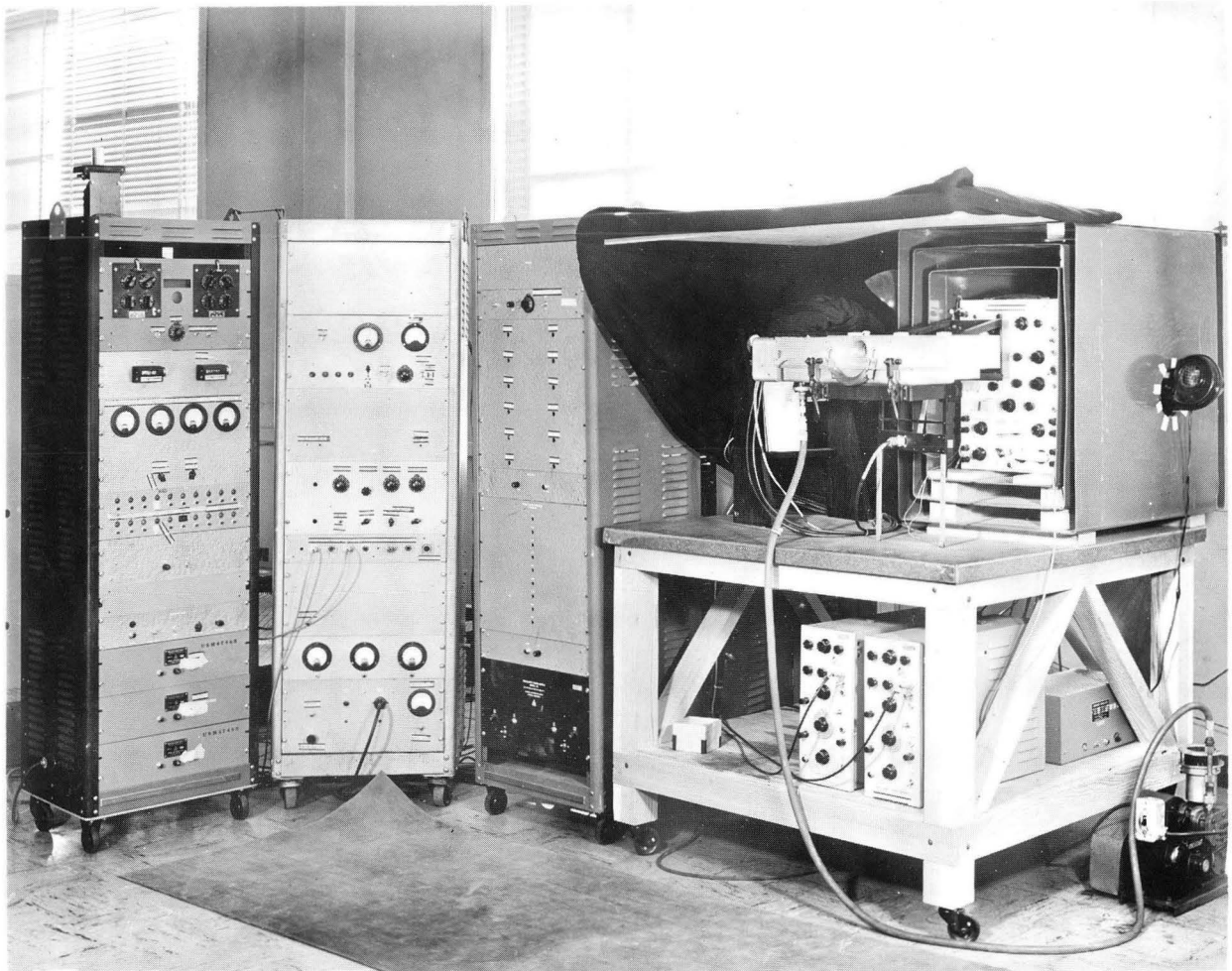


Fig. 9. Signal-programming and recording equipment.

Z N - 1165

(FILE NO. 15370-8)

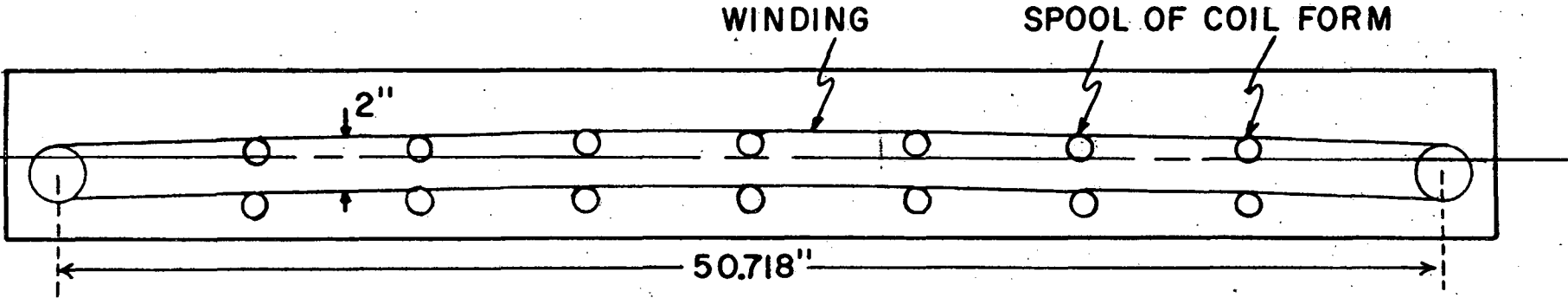


FIG. 10 DIAGRAM OF KIDNEY COIL

ZN-1166

### F. n-Coils

Although the balanced kidney coils provided a means of studying radial variations of flux density, the greater precision and convenience offered by a set of coils designed specifically for this purpose led to the construction of the so-called n-coils. This set of coils consisted of two long, narrow coils mounted on a base plate with their centerlines parallel and separated two inches radially; the assembly extended azimuthally over two sectors. The coils were connected in series-opposing, and a third small coil was added to make the effective areas of the opposing coils equal within about 0.005%. Connections between the coils were made locally, only the difference signal being brought out through a cable; this arrangement is of considerable advantage over remote mixing of the signals wherein cable capacitance may introduce errors in the difference signal. The n-coil assembly was calibrated in terms of radial gradient in a portion of the bevatron field that had been studied, for this purpose, with the kidney coils. In use, the area balance of the n-coils was checked frequently by observing the effect of inverting the assembly. For studying the radial gradient of the flux density, the n-coils were very satisfactory;  $n$  was measured with an accuracy of about 4% and a survey was made covering at least 162 positions in each quadrant.

### G. Verticality Coils

In measuring the radial component of flux density, it is necessary to define and select that component by accurate angular positioning of the detecting element. The lines of flux in the usable portion of the bevatron's field curve with a radius of about 1,000 inches; thus, to determine the location of the median surface to 0.1 inch, a precision in angular position of  $10^{-4}$  radian is required. To provide this precision in positioning a search coil, a special "verticality coil" assembly was made. Three coils, each of about  $3.8 \times 10^5$  turns-cm<sup>2</sup> area, were cast in a block of epoxy-type resin. They were approximately coplanar, with centers in line two inches apart. The effective areas of the coils were made coplanar within  $10^{-4}$  radian by adding turns of wire as trimmers. This block was suspended, with the coils in a vertical plane, on two phosphor bronze wires; the plane of the coils was adjusted to hang within  $10^{-4}$  radian of vertical and the wires preserved the same angle with respect to vertical within  $10^{-5}$  radian. The coils were immersed in a bath of insulating oil to damp their swinging motions. This assembly was inserted in the bevatron gap with the plane of the coils perpendicular to the radial direction, and measurements of radial components of the dynamic field at three points across the gap were possible. Corrections were made for the errors in angle of the coils, and this angle was checked frequently by observing the change in signal introduced by rotating the assembly  $180^\circ$  about the vertical axis. Location of the median surface was calculable from these radial-component data combined with the results of the residual-field radial-component measurements.

#### H. Special Survey Coils

To explore the region between the outer-radius wall of the vacuum tank and the outer leg of the magnet yoke, a special thin coil was constructed. Access to this region was through the magnet-winding ventilating slots in the yoke. So that the coil could pass through these slots it was made in the shape of a flat disk  $3/16$  inch thick and 3 inches in diameter.

In the target region at the exit end of Quadrant 2, a survey of the fringing field was made. One-inch-diameter search coils were used here. Many point measurements were made from which it was possible to obtain the shape of the fringing field.

## DESCRIPTION OF BEVATRON FIELD

A. Average Flux Density

A basic item in most magnet studies is the dependence of flux density upon exciting current. This curve for the bevatron magnet is given in Fig. 11. An estimated error of  $\pm 1/3\%$  is associated with the results of average flux-density measurements. In a magnet having straight sections, fringing of the field at the quadrant ends, requires special consideration in calculating particle frequency and energy as a function of flux density. The boom-coil measurements provided information that allowed calculation of the effective magnetic length of a quadrant. This length is defined by the equation

$$\text{effective length of quadrant} = \frac{1}{4 \langle B \rangle} \oint B dl,$$

in which  $\langle B \rangle$  is the average flux density in a typical midquadrant sector and the line integral of flux density is taken through one complete turn along the gap centerline. In the bevatron, the effective length exceeds the mechanical length of a quadrant by an amount depending upon the flux density. This amount is 2.5 inches at injection, increases to a maximum of 8 inches at 3,000 gauss, then falls to less than 1.0 inch near peak field. The pole tips at the quadrant ends each had been cut back 5 inches to alter the fringing field. Because model measurements yielding this dimension were not considered very precise, these results on the bevatron are more satisfactory than could reasonably have been expected.

Studies of the azimuthal variation of flux density revealed that the field in the center two sectors of each quadrant was consistently about 5 gauss higher than average. The vacuum tank structure in these sectors is not typical of the sectors in general, and the effect on eddy-current distribution may explain the 5-gauss anomaly observed. A correction was made to the magnetic field by currents induced in the pole-base windings of the center sectors; measurements showed that the desired result of removing the inhomogeneity had been attained. Other azimuthal variations were small and, except for quadrant end effects, random in distribution. As measured with the kidney coils, the flux density of most of the sectors was within 0.2% of the average at all values of magnet current.

B. Radial Variation of Flux Density

The behavior of the field exponent  $n$  as a function of flux density and radius displays some interesting features. Figures 12 and 13 give the radial variation of  $B$  and of  $n$  at several values of flux density. It is seen that at the lower flux densities,  $n$  drops to below 0.4 near the outer region of the magnet aperture. These low values of  $n$  appeared somewhat unexpectedly in the bevatron field; however, two aspects of the model measurements which bear upon this must be noted here. Whereas in the full-scale machine the local variations in  $n$  are apparent, measurement and analysis of the model did not show these features nearly as clearly or as accurately. The second item concerns the raised portion at the outer edge of the pole tips; in the 1/7-scale model, the height of this outer raised portion was proportionately less than called for in the full-scale tips. Considering these facts, it is difficult to compare in great detail



(FILE NO. 15370-9)

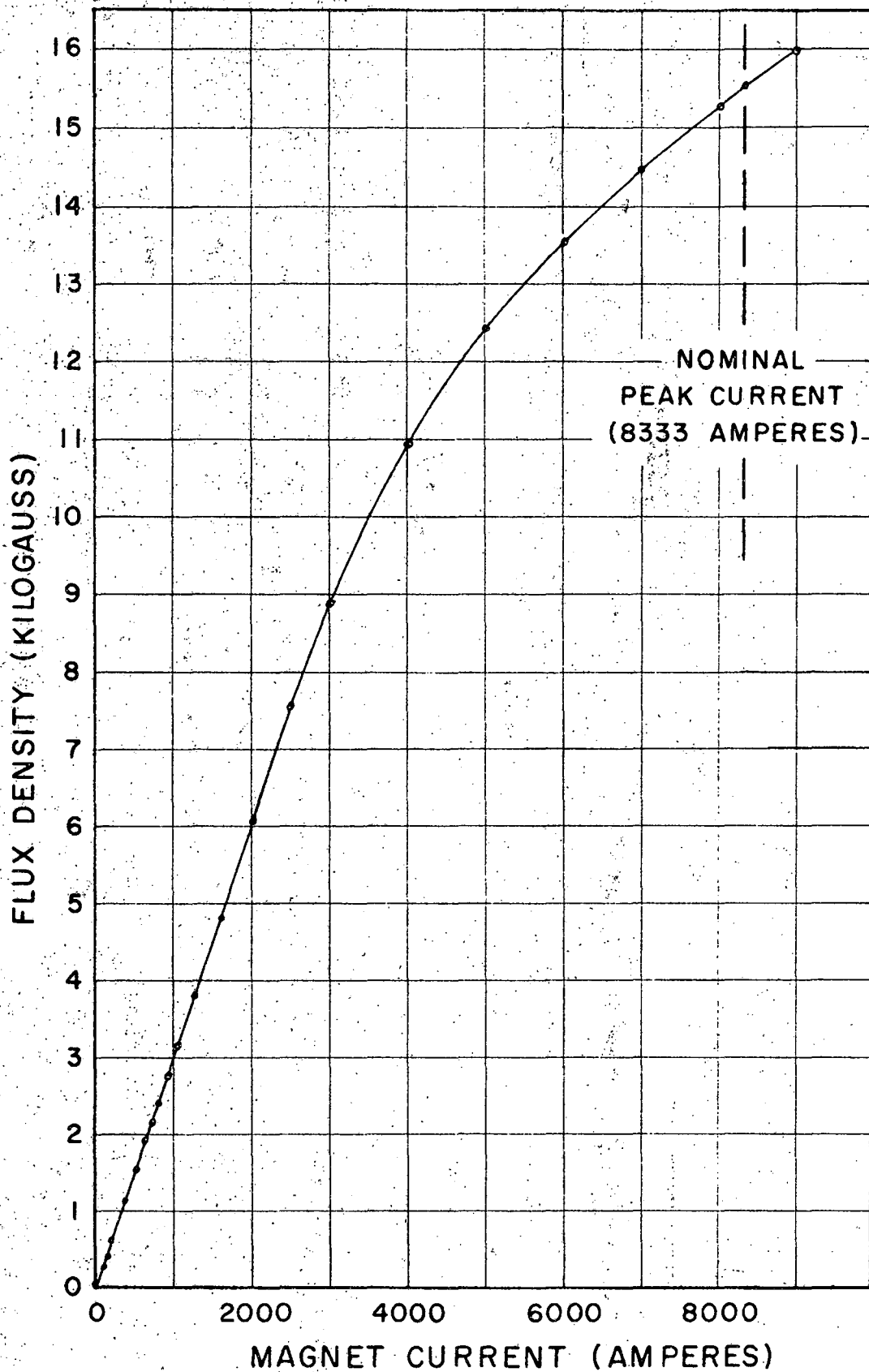


FIG. II AVERAGE FLUX DENSITY AT GAP CENTERLINE

(FILE NO. 15370-10)

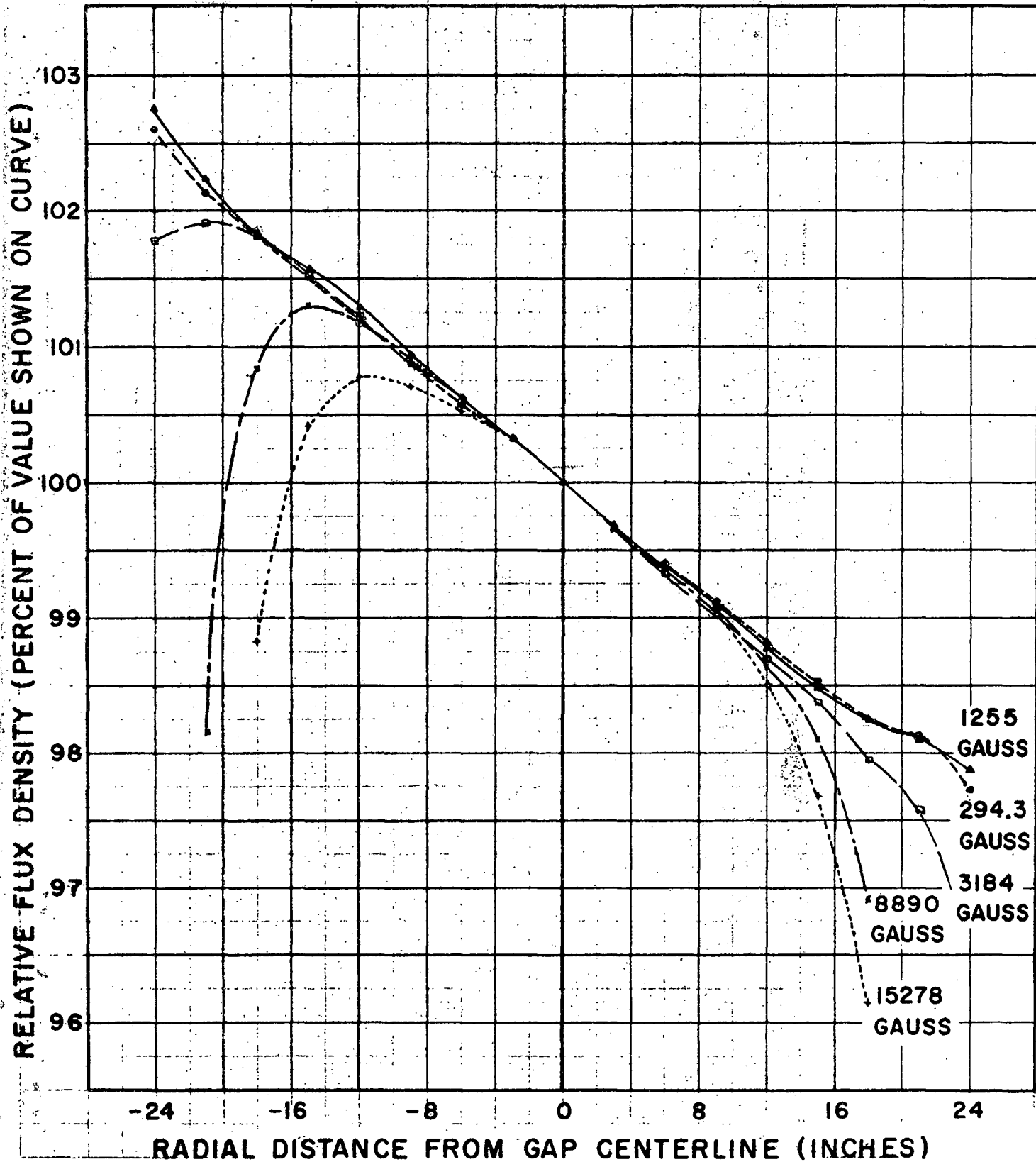


FIG. 12 RADIAL VARIATION OF FLUX DENSITY

(FILE NO. 15370-11)

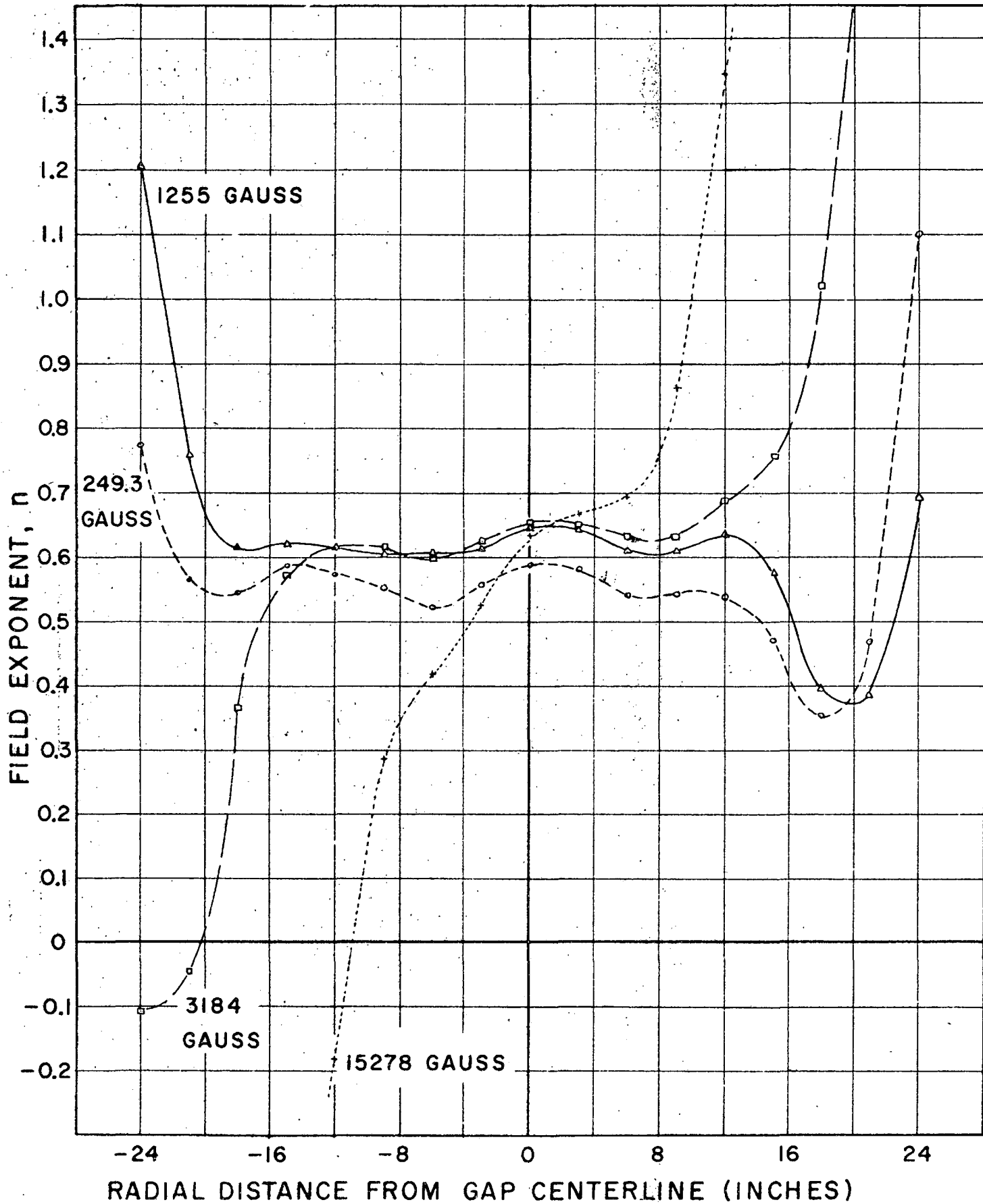


FIG. 13 FIELD EXPONENT  $n$  VERSUS RADIUS

### ACKNOWLEDGMENTS

The magnet tests were carried out with the valuable aid and cooperation of many persons. For their advice and assistance the author is indebted to Mr. William M. Brobeck, Mr. Charles G. Dols, and Dr. Wilson M. Powell. Included among those concerned with the equipment design and construction and the execution of the measurements were Joseph H. Dorst, Walter K. Nelson, Arthur E. Sherman, and Peter G. Watson.

the model and the full-scale behavior of  $n$  versus radius. A resonance at  $n = 0.5$  between radial and axial particle oscillations makes this region of low  $n$  effectively unusable for guiding particles during acceleration. A correction of this feature seemed desirable when the measurements were in progress; accordingly, a pole-face-winding circuit was set up that would introduce induced currents of the desired distribution. Measurement of the altered radial gradient showed that the correction obtained was in agreement with the calculated effect expected, and that during the critical injection period the unusually low values of  $n$  had been removed. The average value of  $n$  is generally lower at injection than at higher flux densities. This behavior was also observed in the magnet model, and at that time the amount of taper of the magnet gap was increased to avoid trouble at injection with the  $n = 0.5$  resonance. In the original design the taper corresponded to  $n = 0.60$ ; the increased taper corresponds to  $n = 0.63$ . Recently, in the course of the bevatron operation, pole-face-winding currents have been introduced which increase the value of  $n$  at injection by a calculated increment of 0.1 over most of the gap; this action has yielded considerable improvement in the apparent stability of the beam shortly after injection. From this evidence, one is led to suspect that disturbing resonance phenomena were being encountered with the injection field shown in Fig. 13. The generally low value of  $n$  at injection may arise from the eddy-current distribution in the vacuum tank; the tank is not symmetric about the gap and the qualitative effect of this coincides with the observed depression in the field exponent.

A study of resonance phenomena in terms of the field exponent  $n$  allows one to define the radial interval within which the field is usable for particle acceleration. The resonance at  $n = 0.5$  and other resonances near  $n$ -values of 0.77 to 0.8 have led to the adoption of the criterion  $0.53 < n < 0.73$  to define the "usable" field. The radial extent of the usable field is obtained from  $n$ -versus-radius curves and may be studied as a function of flux density. See Fig. 14.

As the flux density rises, saturation of the iron in the pole tips brings about a reduction in the width of the usable field region until only nine inches remain at 15,000 gauss. At injection, a large usable aperture is required; however, damping of the particle oscillation amplitudes as the flux density increases should make a progressive reduction of aperture acceptable. Considering this and the desirability of obtaining as high a flux density as possible at the nominal peak current, triangular cutouts were made in the pole-tip laminations (see Fig. 1). Before saturation of the iron at the pole-tip edges, the effect of the cutouts is not seen in the magnetic field. At higher flux densities, the cutouts result in an increased flux density at gap center and some reduction in the width of the usable field region. Operating experience with the bevatron has not yet provided a conclusion as to the over-all desirability of the pole-tip cutouts.

The curves of  $n$  versus radius in Fig. 13 show a consistent wavelike characteristic, which is found throughout the magnet. One can explain this by noting a detail of the construction of the laminated pole tips. The outer laminations are of graded lengths, making the tip broader at the radially outward end. The ends of these shorter laminations occur at intervals across the gap and cause the waves seen in the  $n$ -versus-radius curve.

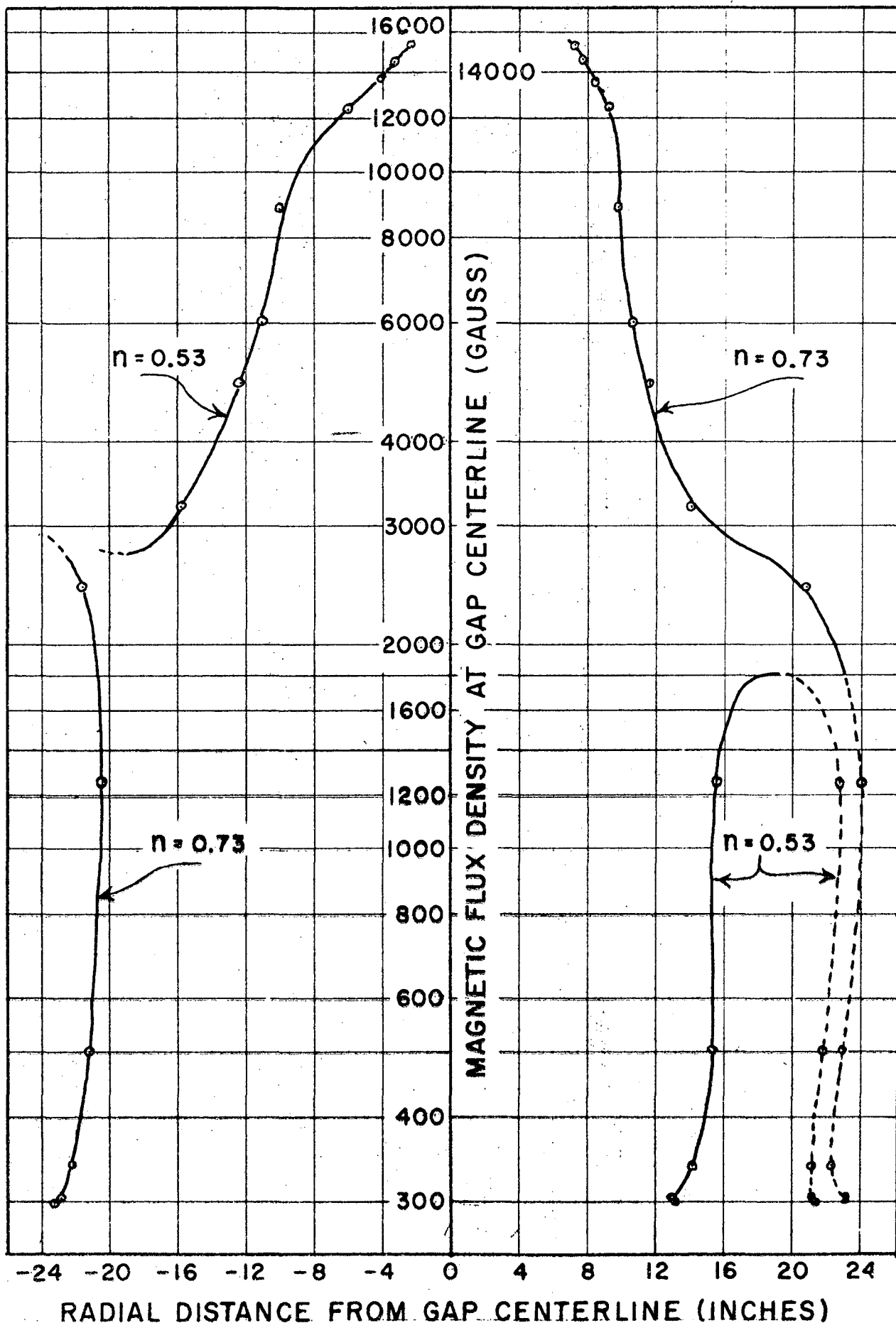


FIG. 14 RADIAL LIMITS OF MAGNETIC FIELD FOR WHICH

$$0.53 \leq n \leq 0.73$$

### C. Effect of Pole-Face-Winding Currents at High B

The pole-face windings were tested in the 1/7-scale magnet model. Effects produced at low flux densities in the gap were in quite good agreement as to amplitude and distribution with what one calculates assuming iron of very high permeability. Predictability of the pole-face-winding effects was again confirmed by our success in the first trial at altering the bevatron injection field. Model measurements at high flux densities suffered from lack of precision, and further measurements at peak magnet current were included in the full-scale tests. Currents up to 1,200 amperes were passed through the windings and the results studied at 15,500 gauss flux density. The effect of the pole-face windings was not greatly altered by the partially saturated condition of the pole tips; differences in distribution and amplitude not exceeding 25% were found. Pole-face-winding effects at various radii exhibit differences that are consistent with the limited radial dimensions of the gap. To the precision of our measurements the effects are linearly dependent upon winding current. The results of the pole-face-winding experiments at high flux density, in the form of graphs of the measured field perturbations are available from the UCRL Magnet Testing Group.

### D. Median Surface

Results of the horizontal-component measurements were very gratifying. At most points, the median surface was within 0.2 inch of the mid-gap plane. Except for a possible azimuthal harmonic of about 0.1 inch amplitude at injection, no significant azimuthal features appeared. Limited studies of the radial variation suggest that average deviations of 0.1 to 0.2 inch might emerge from a more complete statistical analysis. In the time since the testing program ended, the positions of the sectors have been adjusted to compensate for settling; however, no subsequent magnetic measurements of median surface have been made.

### E. Miscellaneous

Special interest in the target region at the exit end of Quadrant 2 led to the preparation of a contour map of the fringing field in that region at nominal peak magnet current. (UCRL-Dwg. No. 4Q5394.) The map is large enough to be useful in plotting particle trajectories.

Along the centers of two typical sectors, the field was surveyed from the outer wall of the vacuum tank to the outer yoke. At peak gap flux density, the field in this region has been plotted versus radius. The flux density decreases smoothly with radius, passes through zero and reaches about minus 1,000 gauss at the outer yoke.

Protons being injected into the bevatron are deflected by the stray field occurring along their trajectory. Measurements indicated that at most places this field was less than two gauss; making allowance for the deflection produced by the small field at injection was no problem.

For equipment design and general work around the bevatron, the peak stray field of the magnet cannot be neglected. Reflecting the saturation of the magnet iron, the stray field generally rises at an increasing rate as

the current rises. The intensely peaked pulse of stray field so produced is in contrast with the uniformly rising pulse of field in the magnet gap. The stray field corresponding to nominal peak current was measured at places where electronic equipment was to be located. Magnetic shielding of many components was found to be necessary. A good over-all survey of the stray field in the bevatron building has not yet been made, but from scattered measurements we can assign approximate values to the peak flux density at some points around the magnet. Between the magnet and the wall of the building, these approximate values would be: 20 gauss just inside the building (~40 feet from magnet), 100 gauss about 15 feet from the magnet, and almost 1,000 gauss next to the iron of the magnet yoke.

### SUMMARY

The use of specialized programming and recording equipment was a feature of the bevatron magnetic field measurements. Efforts spent in preparing this equipment resulted in considerably less time spent in recording and reducing data. Specialized search coils also demonstrated their value in yielding information on selected features of the field.

Methods of difference measurement simplified the problems of studying field variations and gradients; as a measurement instrument, the integrator with balanced, opposing search coils is one of the most versatile for these applications.

The most reassuring test of the suitability of the field distribution produced in the magnet has been successful acceleration of protons in the bevatron. One was encouraged to anticipate this outcome by the general acceptability of the field as demonstrated in the magnet-testing program. With the exception of a deficiency at injection (which was corrected by use of the pole-face windings), the bevatron field was in good agreement with predictions based on model tests.

Limited model experience in connection with azimuthal uniformity, effective length, and median surface made the satisfactory results in these areas particularly gratifying.

In planning the measurement program, a selection was made from the many aspects of the magnetic field, of those items to be investigated. Not included in this selection was a survey of the field in the filler-frame space in the vacuum tank. Questions received about this region indicate that a limited survey would have been useful. The measurement of median surface relative to magnet gap would have been more complete if accompanied by a survey of the relative positions of the sectors. Only a very small amount of data was collected on the dependence of residual field upon magnet history; questions about this complex behavior have arisen and more information would be desirable. More specialized questions about the magnet will, of course, arise. Nevertheless, data provided by the measurements program will continue to provide a useful and reasonably adequate picture of the bevatron magnet.



### ACKNOWLEDGMENTS

The magnet tests were carried out with the valuable aid and cooperation of many persons. For their advice and assistance the author is indebted to Mr. William M. Brobeck, Mr. Charles G. Dols, and Dr. Wilson M. Powell. Included among those concerned with the equipment design and construction and the execution of the measurements were Joseph H. Dorst, Walter K. Nelson, Arthur E. Sherman, and Peter G. Watson.